

Article

Designing a Multi-Output Power Supply for Multi-Electrode Arc Welding

Jingzhang Zhang, Shujun Chen, Hongyan Zhao, Yue Yu * and Mingyu Liu

Faculty of Materials and Manufacturing, Beijing University of Technology, Beijing 100124, China

* Correspondence: yuyue@bjut.edu.cn

Abstract: Multi-output power converters using different architectures can have significant efficiency advantages. This paper proposes a multi-output welding power supply that is based on the middle DC converter distributed architecture. This machine includes two converter groups, and each group comprises a three-phase rectifier unit, a full-bridge converter unit, a HF (high frequency) transformer, a rectifier unit, and a chopper converter unit. Among these units, the three-phase rectifier unit, full-bridge converter unit, HF transformer, and rectifier unit convert three-phase AC voltage into a low voltage, and the chopper converter unit converts the low voltage into the required current. The welding power supply can output four DC and two AC currents. This paper also analyzes the stability of the welding power supply. Finally, a prototype is designed and verified through experiments, and the maximum output of the prototype is 300 A. The experimental results show that the converter can output different DC and AC currents according to the requirement, the multiple outputs are independent of the others, and the output phase and value are independently adjustable. After verification, the proposed multi-output welding power supply can output steady current according to the requirement.

Keywords: chopper converter; welding supply; closed-loop control; multi-output



Citation: Zhang, J.; Chen, S.; Zhao, H.; Yu, Y.; Liu, M. Designing a Multi-Output Power Supply for Multi-Electrode Arc Welding. *Electronics* **2023**, *12*, 1702. <https://doi.org/10.3390/electronics12071702>

Academic Editor: Adel M. Sharaf

Received: 18 February 2023

Revised: 29 March 2023

Accepted: 31 March 2023

Published: 4 April 2023



Copyright: © 2023 by the authors. Licensee MDPI, Basel, Switzerland. This article is an open access article distributed under the terms and conditions of the Creative Commons Attribution (CC BY) license (<https://creativecommons.org/licenses/by/4.0/>).

1. Introduction

Welding technology plays an important role in the manufacturing industry, with the rapid development of the industries of aerospace, petroleum processing, marine engineering, energy engineering, etc. It has been put forward to realize the requirements of high-efficiency and high-quality welding production and processing. The arc welding process has been a long-term research field among many researchers, who have always aimed to develop new high-quality and high-efficiency welding techniques [1–3].

Long-term research has shown that single-electrode welding efficiency can be achieved through the use of external magnetic fields, waveform control, or altering shielding gas composition, thereby improving welding performance. However, these efficiency-boosting approaches often increase production costs, equipment complexity, and poor compatibility between devices, and therefore have not achieved significant breakthroughs in efficiency. Recently, a variety of new arc welding processes have emerged, such as the tandem welding process [4], double-sided double arc welding process [5], bypass electrode GMAW (gas metal arc welding) welding process [6], multi-electrode argon arc welding process [7], and cross-coupled arc welding process [8].

Compared to the traditional welding process, which only needs two electrodes to provide one current, these welding processes are collectively based on the multi-electrode arc welding technology, which use more than two electrodes to provide two or more currents to weld, thus significantly breaking through the limitations of the traditional welding process and providing new technical means for achieving high-quality and high-efficiency arc welding. Currently, the following are the main multi-electrode arc composite welding processes in use:

1. Tandem welding process

As shown in Figure 1, the tandem welding process employs dual independent power supplies, integrating two welding wires into a single welding torch, each powered by a separate welding power source. The two arcs can be independently adjusted and are arranged in a front-to-back structure. The melting of both wires compensates for any inadequacies in the filling of the weld seam. This not only increases the metal deposition rate, but also enables high-speed welding [4].

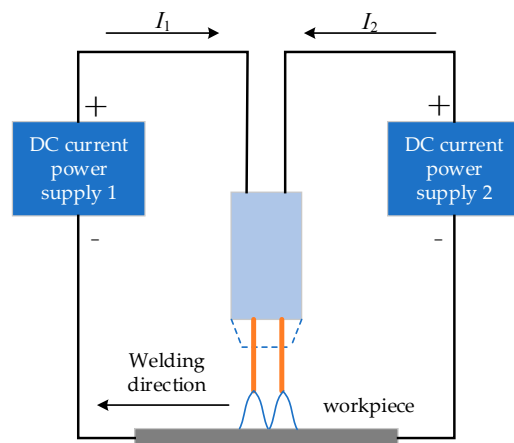


Figure 1. Tandem welding process.

2. High-speed triple-wire gas metal arc welding process

As shown in Figure 2, high-speed triple-wire gas metal arc welding is similar to the tandem welding process. The three welding wires are arranged longitudinally as the leading wire, the intermediate wire, and the trailing wire. Each wire has an independent welding system with its welding process parameters controlled separately to meet various welding requirements [9–11].

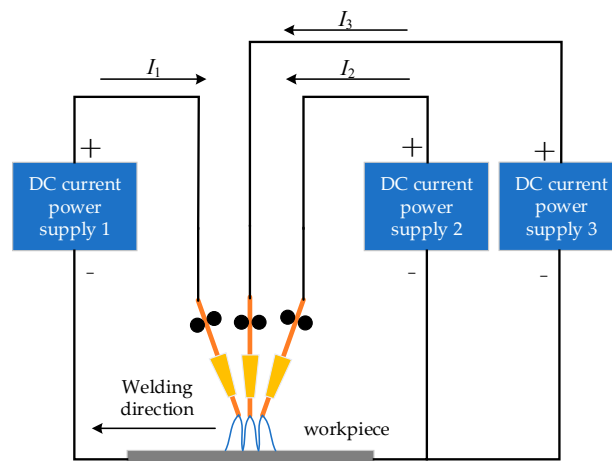


Figure 2. High-speed triple-wire gas metal arc welding process.

3. Bypass GMAW process

As shown in Figure 3, the bypass GMAW process utilizes a bypass electrode to reduce the heat input to the workpiece while ensuring wire melting efficiency. A portion of the total wire current is shunted through a GTAW (gas tungsten arc welding) torch, maintaining the wire deposition rate while reducing the heat input to the base material. By adjusting the bypass arc current, the desired distribution of heat between the wire and the base material can be achieved [12–16].

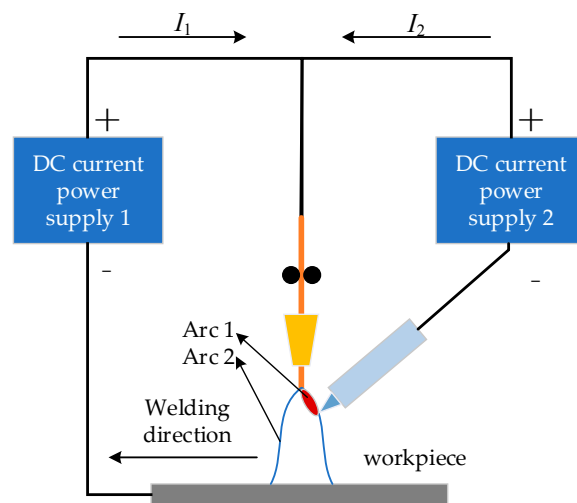


Figure 3. Bypass GMAW process.

4. Dual-wire dynamic triple-arc welding process

As shown in Figure 4, the dual-wire dynamic triple-arc welding method involves alternating the formation of two arcs between the two welding wires and the workpiece, while the indirect arc between the two wires switches polarity based on the arc changes between the wires and the workpiece [17–19].

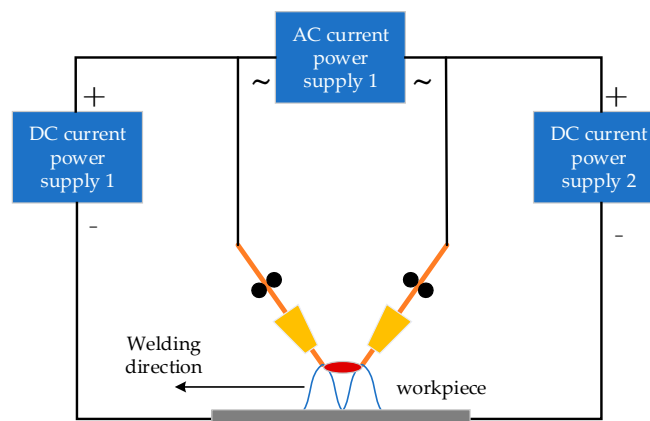


Figure 4. Dual-wire dynamic triple-arc welding process.

5. Cross-coupling arc welding process

As shown in Figure 5, cross-coupling arc welding is based on forcibly cross-coupling non-consumable electrode arcs and consumable electrode arcs within a limited space. The main arc is established between the main welding torch and the workpiece, dominantly determining the input of arc heat and arc force to the workpiece, with part of its heat melting the welding wire. The inter-wire arc burns between the two welding wires without electrical connection to the workpiece, mainly controlling the mass transfer and supplementing part of the heat input to the workpiece [3,19–21].

The above five processes are the most commonly used multi-electrode arc welding processes. By observing the principles of these processes, it can be found that they all involve the combination of multiple different types of welding power sources. These welding processes are composed of three or more electrodes with DC or AC current. According to different process requirements, different welding power sources are combined with different welding processes.

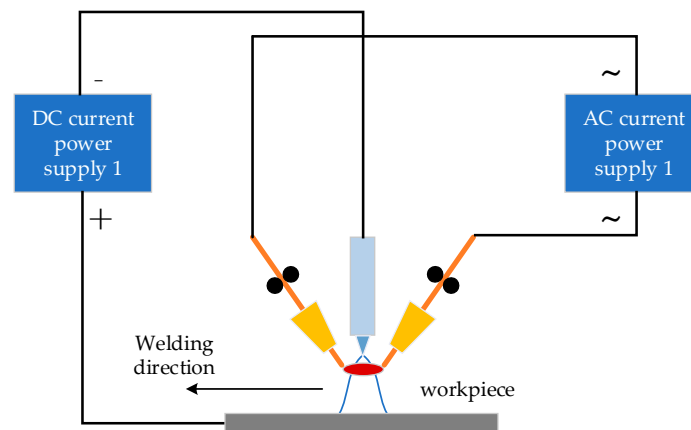


Figure 5. Cross-coupling arc welding process.

In order to realize a multi-electrode welding process of multiple combinations, the acquisition of numerous welding power sources is necessary, resulting in a significant increase in cost and impact on production efficiency. Consequently, there is a significant need for a multi-electrode welding power supply that can be flexibly and conveniently combined into various welding processes.

Therefore, the power supply designed in this paper can use single power supply to meet the combination requirements of each process. A combination of different welding processes can be achieved through different combinations of multiple electrodes. This power supply is easy to use, low-cost, and offers a simple, yet effective, control method.

In this paper, by employing an independently controlled topological structure, we introduce the concept of multi-output, multi-electrode arcs, enhancing the energy utilization rate of the power supply, and enabling the implementation of various welding processes on a single independent power source. The power supply control system collects arc current signals through the current sampling unit and feeds back the preset control parameters to the power supply control unit to achieve precise current control, further advancing the development of high-quality, efficient arc welding processes.

2. Converter Structure and Working Principles

2.1. Multiple Output Converter

This paper proposes a welding power-supply system for a multi-output welding process, as shown in Figure 6. As shown in Figure 6, i_{g1} , i_{g2} , i_{g3} , and i_{g4} are the target current values and v_{g1} and v_{g2} are the target voltage values; these values are output by the controller. The actual current values are i_{o1} , i_{o2} , i_{o3} , and i_{o4} , and v_{o1} and v_{o2} are the actual voltage values.

This machine includes two converter groups, and each group comprises a three-phase rectifier unit, a full-bridge converter unit, a HF transformer, a rectifier unit, and a chopper converter unit. In order to reduce the impact on the power grid, we have added an AC 3-Phase 4-Line Filter module to the grid input side of the constant voltage source, which can effectively reduce the impact. The three-phase rectifier unit converts 380 VAC to 540 VDC, and the full-bridge unit produces 20 kHz pulse waves for the HF transformer, for which the turn ratio is 14:3. After the rectifier unit, the voltage becomes 50 VDC. During the welding power supply, the voltage is constant. The chopper converter unit is the most important part for the power supply, as shown in Figure 5. In order to demonstrate, this paper uses different colors to indicate different outputs. In Figure 7a, the red line and blue line represent two DC currents, respectively. In Figure 7b, the red line and blue line represent the different current directions in AC mode. In Figure 7c, the red line and blue line represent the different current directions in AC mode, and the green line represents the DC current. Figure 8 shows the working principle of the IGBT in each mode, and the colors corresponded with Figure 7. The chopper unit can output two DC currents or one

AC current according to the requirement. The two groups use one controller to control the current; thus, the output current can be more flexible than the traditional multi-output welding power supply. Therefore, the combination of the two groups of converters can output four DC and two AC currents.

The power supply this paper designed can output four DC currents or two AC currents. Since the maximum output current and voltage are 300 A and 35 V, the maximum power of each output is 10.5 kW. Therefore, the maximum power of the constant voltage source is 42 kW. According to the power standard, this maximum power is too big for the author’s lab to design the chopper circuit. Due to that, this paper used two constant voltage sources to provide the power. Each group is designed as the middle DC converter distributed architecture of the multi-output power supply. If the constant voltage power is enough, the two groups can be changed to one and more chopper circuits can be added to realize more outputs.

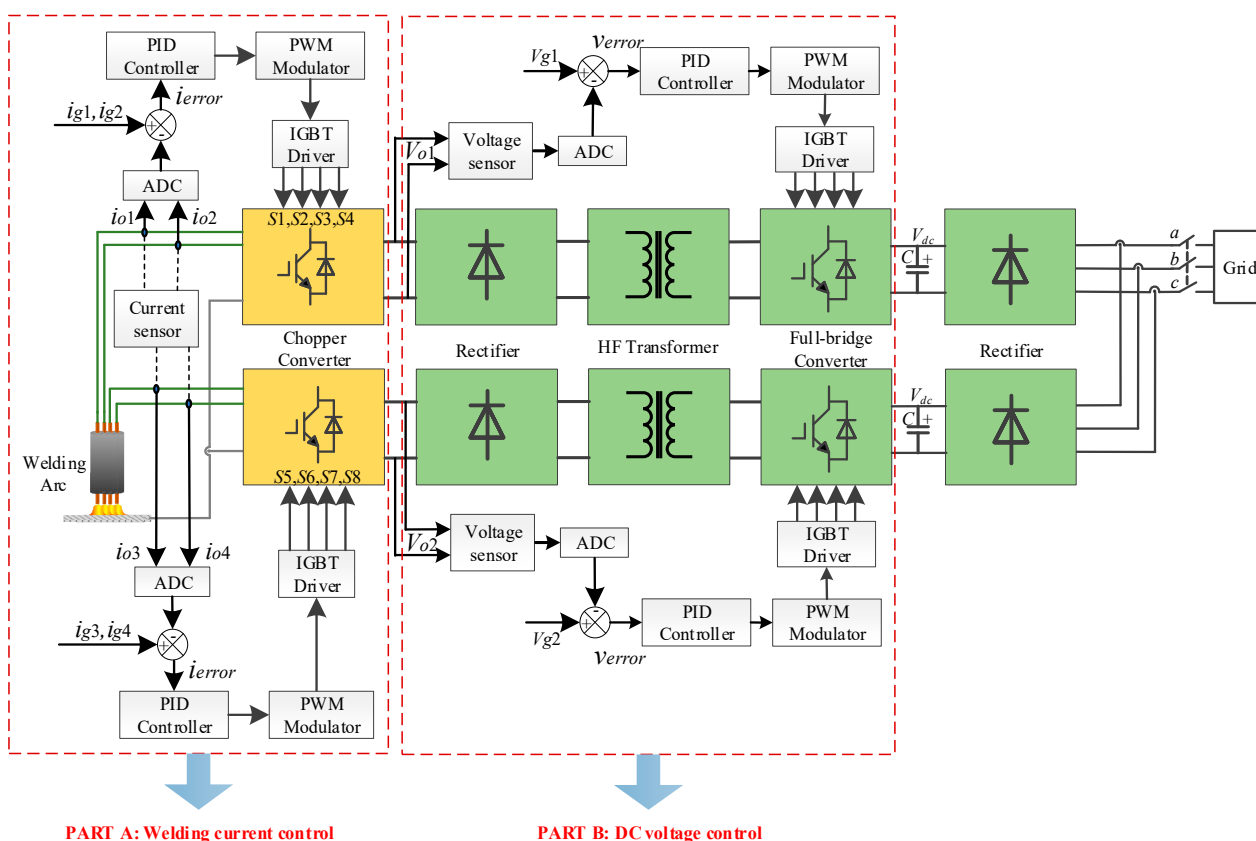


Figure 6. Multi-output welding power-supply system.

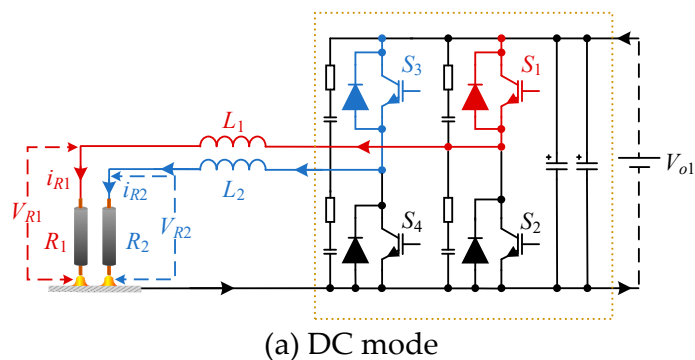


Figure 7. Cont.

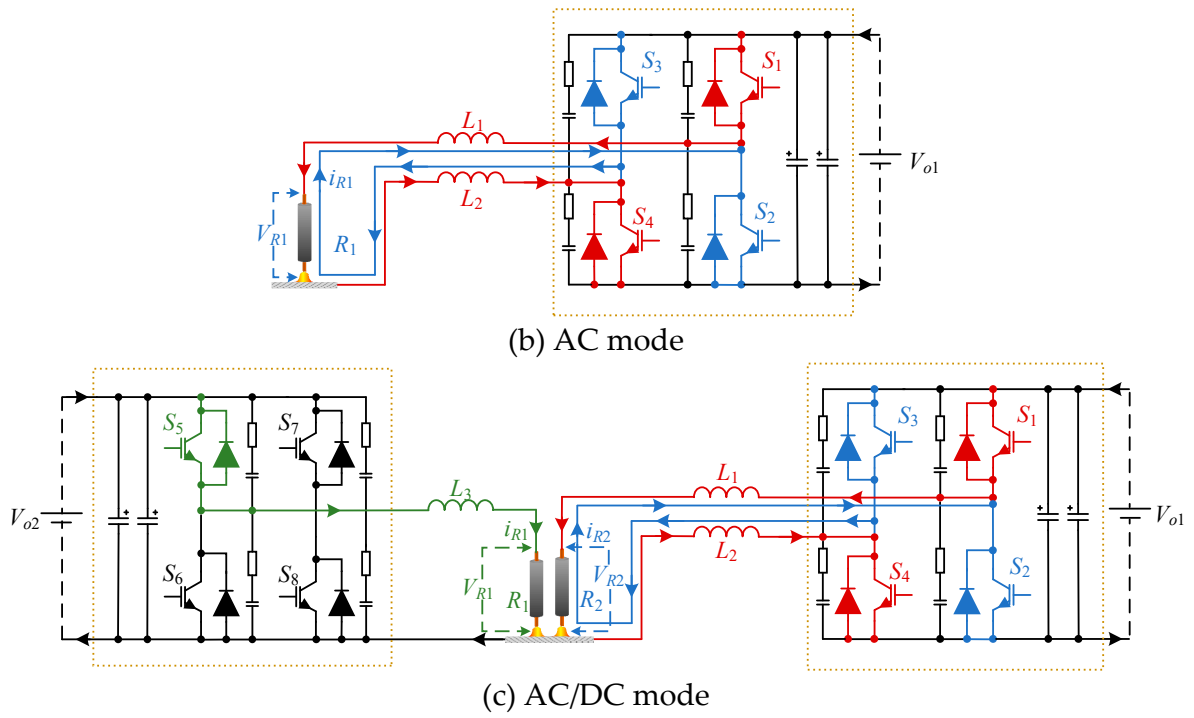


Figure 7. Chopper converter working principles.

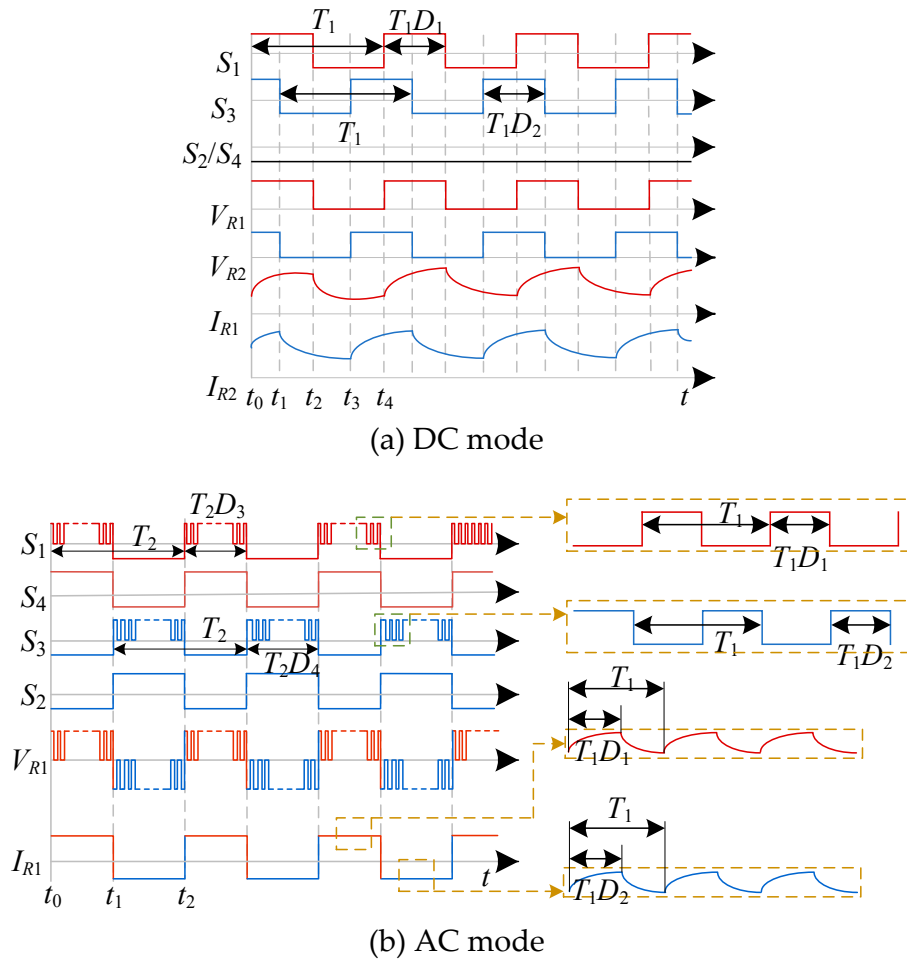
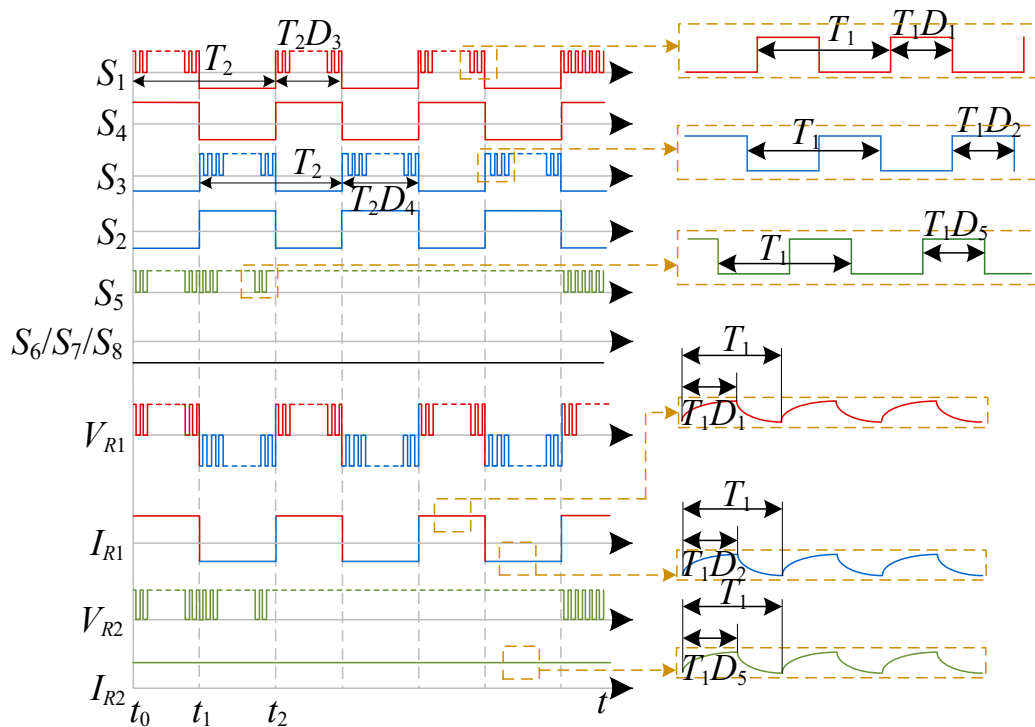


Figure 8. Cont.



(c) AC/DC mode

Figure 8. Switching diagrams.

2.2. Converter Working Mode Analysis

Owing to the existence of an inductor, the output current is constant. During the welding period, the welding current and voltage are constant. Thus, the welding arc can be regarded as a resistance, and the resistance only slightly changes within a certain range.

2.2.1. DC Mode

In DC work mode, when the switches S_1 and S_3 turn on and off, the DC voltage is chopped, and the inductors L_1 and L_2 work in continuous conduction mode (CCM); the current through the resistance is DC current. The working principle is shown in Figure 7a. The specific waveform is shown in Figure 8a. $T_1 = 50 \mu s$, and D_1 and D_2 are the duty cycles; the value is due to the current.

At t_0 , S_1 and S_3 turn on. Currently, the current on the arc resistance R_1 goes from V_{o1+} through S_1 , L_1 , and R_1 to V_{o1-} . Moreover, the current on the arc resistance R_2 goes from the voltage V_{o1+} through S_2 , L_2 , and R_2 to the voltage V_{o1-} . The energy in the circuit is stored by the inductors L_1 and L_2 , and the current increases.

At t_1 , S_1 is still on, and S_3 is off. At this time, the inductor L_1 continues to store energy and the current on R_1 continues to increase. Since S_3 turns off, L_2 discharges energy to prevent the current from changing, and the current decreases.

At t_2 , S_1 turns off, and S_3 is in the off state. The energy stored in the inductors L_1 and L_2 is discharged to keep the current on the arc resistances R_1 and R_2 stable and continuous.

At t_3 , S_3 turns on, S_1 remains off, the inductor L_2 is charged and the current through the arc resistance R_2 begins to increase. Furthermore, the current on the arc resistance R_1 continues to decrease.

At t_4 , both S_1 and S_3 are on, such as at time t_0 .

2.2.2. AC Mode

As shown in Figure 7b, when the converter is in AC mode, the welding power supply outputs forward and reverse currents. During the welding process, the frequency of the AC current is 40~50 Hz. Therefore, in the AC mode, one AC cycle can be regarded as two

DC modes. The two DC modes are forward current and reverse current, and the specific working waveform is as shown in Figure 8b. T_2 is the period of AC welding, and D_3 and D_4 are the forward times of AC welding.

At time t_0 , S_1 and S_4 turn on simultaneously and the current goes through V_{o1+} , S_1 , R_1 , and S_4 to V_{o1-} . When in AC forward operation, S_1 turns on and off at a frequency of 20 kHz, and S_4 is always in the on state. Therefore, this state can be considered the same as the DC state.

At time t_1 , in AC mode, the current changes from forward to reverse, and S_1 and S_4 turn off. Then, after a dead time of 5 μ s, S_2 and S_3 turn on. The current goes through V_{o1+} , S_3 , R_1 , and S_2 to V_{o1-} . In AC reverse operation, S_3 turns on and off at a frequency of 20 kHz, and S_2 is always in the on state. The state at this time can be regarded as the DC state.

At time t_2 , S_2 and S_3 turn off, and S_1 and S_4 turn on. At this point, a full AC cycle is completed.

2.2.3. AC/DC Mode

When working in AC/DC mode, one group of converters provides AC output and the other provides one or two DC outputs as required, as shown in Figure 7c. Figure 8c shows the working waveforms. D_5 is the forward time of AC current.

In AC/DC mode, the converter can output one or two DC currents and one AC current. Therefore, when the power supply outputs DC current, the working mode is the same as the DC mode, and when the power supply outputs AC current, the working mode is the same as the AC mode. Thus, the analysis is the same as shown in Sections 2.2.1 and 2.2.2. The two modes are simultaneously working to generate two welding arcs.

3. Analysis of the Converter

Unlike ordinary DC/DC converters, for a welding power supply the load is always changing owing to the uneven surface of the workpiece or the shaking of the welding torch in the welding working process. Therefore, it is necessary to analyze the system stability characteristics of the converter [22–26].

For convenience of analysis, the output voltage of each rectifier unit in each group is considered as a constant value U_s . For the single buck chopper circuit shown in Figure 9, suppose the inductor works in CCM. In Figure 9, U_s represents the input voltage, d_0 and d_1 represent the control PWM duty cycle, I represents the output current, L represents the inductor, and R_L represents the load. The IGBT is controlled by the PWM signal to turn on or off, and the output current can be adjusted using the duty cycle. This paper uses a simple linear control method, and its control algorithm uses classic PID control. PID controllers are widely used in the industrial control system. This paper adopts PID as the closed-loop control algorithm due to the stability of PID control. Welding power supplies are industrial equipment; during the welding process, stability is the most important thing, and welding power output closed-loop control is a lag regulation. Therefore, the classical PID algorithm was selected as the closed-loop control algorithm.

The closed-loop control system of the converter is shown in Figure 10, where $G(s)$ is the transfer function from the duty cycle $d(s)$ to the output $I_o(s)$, and $G_i(s)$ is the transfer function of the error between $I_o(s)$ and i_g . $G_m(s)$ is the transfer function of the PWM pulse width modulation, $H(s)$ is the transfer function representing the negative feedback current measurement network, and $G_v d(s)$ is the transfer function of the controller. The closed-loop system block diagram of the buck converter can be represented in a standard form, as shown in Figure 8. The original loop gain function $G_o(s)$ is as follows:

$$G(s) = G_m(s)G_{vd}(s)H(s) = \frac{U_o}{d} \frac{1}{1 + s\frac{L}{R} + s^2LC} \alpha \quad (1)$$

To reduce the influence of the phase margin correction effect, we added the closed-loop PI control algorithm, and then obtained $K_p = 0.03$ and $K_I = 9.6$.

Therefore, the transfer function of the controller is as follows:

$$G_c(s) = \frac{9.6 \cdot (1 + 4.35 \cdot 10^{-3}s)}{s} \tag{2}$$

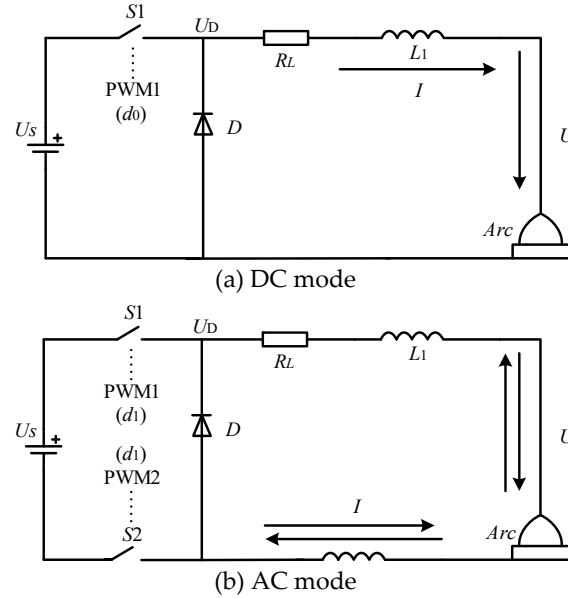


Figure 9. Simplified block diagram.

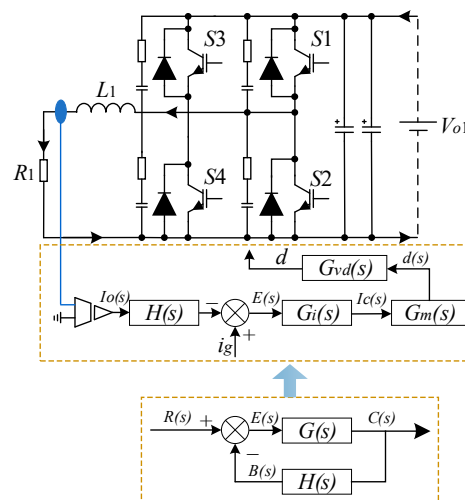


Figure 10. Control block diagram.

By substituting the parameters of the converter into (1), when the output current is 300 A, the output voltage is $U_o = 25$ V, the load is 0.083Ω , and the inductance is $35 \mu\text{H}$. However, in the AC mode, the inductance is $70 \mu\text{H}$. Moreover, the switching frequency is 20 kHz, that is, the switching period is $T = 50 \mu\text{s}$. At this time, the duty cycle of the DC mode is 42%, and the duty cycle of the AC mode is 84%. The closed-loop equivalent transfer function of the system after correction is as follows:

DC:

$$G_o(s) = \frac{9.6(1 + 4.35 \cdot 10^{-3}s)}{s} \cdot \frac{59.62}{100 + 4.22 \cdot 10^{-2}s + 3.5 \cdot 10^{-6}s^2} \tag{3}$$

AC:

$$G_o(s) = \frac{9.6(1 + 4.35 \cdot 10^{-3}s)}{s} \cdot \frac{29.76}{100 + 8.43 \cdot 10^{-2}s + 7 \cdot 10^{-6}s^2} \tag{4}$$

After calculation, the PI parameters K_p and K_i were obtained. The transfer function of the overall system was established in MATLAB, the parameters were substituted into the system, the Bode diagram was obtained, and the Bode diagram was used to judge whether the established system is stable and reliable, and whether the selected device parameters are appropriate. The Bode diagram is shown in Figure 11, and the phase angle margins in the DC and AC modes are 44.2° and 57.1° , respectively, which meet the design requirements.

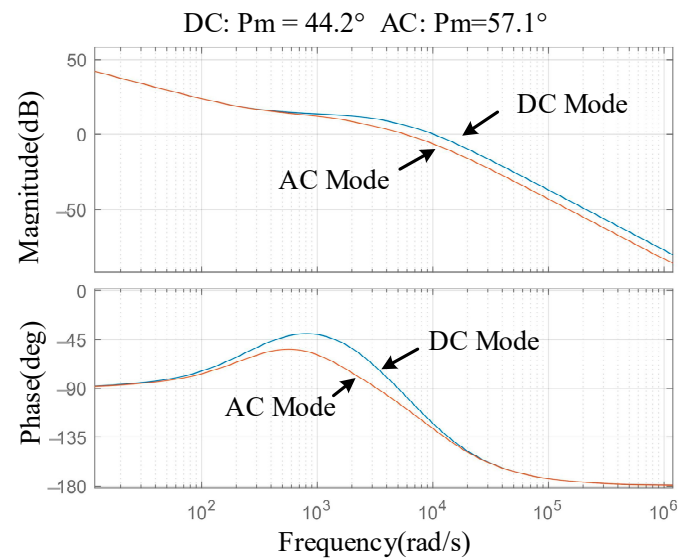


Figure 11. Control part Bode diagram.

4. Experimental

An experimental prototype is shown in Figure 12, and the specific parameters are shown in Table 1. The chopper converter unit input voltage is the rectifier unit output voltage, which was set to a constant voltage of 50 V. The output current could be adjusted from 50 to 300 A. Since the volt–ampere characteristic formula of welding is $U = 10 + 0.05I$, the corresponding output voltage ranges from 12.5 to 25 V. To stabilise the voltage of the rectifier unit output, six 2200 μF electrolytic capacitors are used, and the total capacitance is 13,200 μF . The output inductor value is 35 μH . Several IGBTs are used as the switches of the chopper converter unit. The IGBT model is Infineon FF300R12KS4, and the switching frequency is 20 kHz. A Hall sensor is used to measure the output current. A value of 100 A corresponds to 1 V. The output signal of the Hall sensor is converted by AD and transmitted to STM32F107VCT6 to calculate the PID and output the corresponding PWM. The oscilloscope Agilent DSO7012B is used to acquire the waveforms.

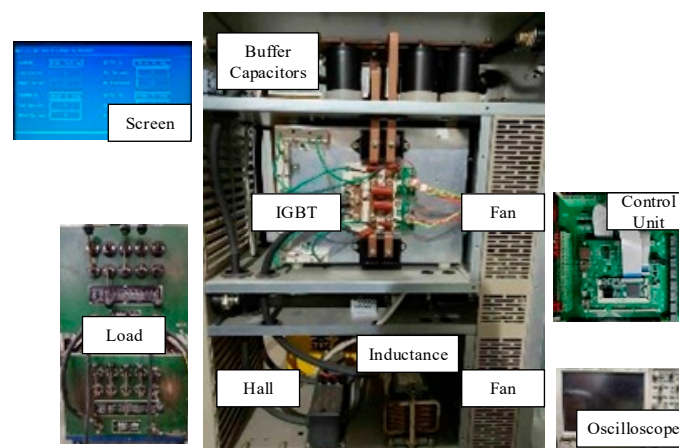


Figure 12. Experimental prototype and experimental conditions.

Table 1. Experimental specifications.

Parameters	Value
Input voltage	50 V
Output Voltage	12.5~25 V
Output Current	50~300 A
Capacitor	2200 μ F–220 V \times 6
Inductance	35 μ H
IGBT	Infineon FF300R12KS4
Switching frequency	20 kHz

The current level increment presented in the table is adjustable by 1 A, ranging from 50 A to 300 A. The selection of 1 A as the increment value was based on the experimental requirements of our study.

Regarding the minimum current level setting of 50 A, it was determined based on the requirements of the welding process under investigation, since currents lower than 50 A are rarely utilized in the industrial welding operations. Furthermore, low current levels, specifically below 50 A, have a higher tendency to interrupt the arc during the polarity change of the AC current. Therefore, setting the minimum current level to 50 A ensures the reliable completion of the welding process while maintaining a stable arc.

The welding process in this system uses the contact arc initiation method. The arc initiation method is both applied in AC and DC mode, and the output current is monitored after the arc is started. To safeguard against the output of welding, the system equips a voltage sensor between the welding electrodes and workpiece. After the arc is initiated, a short circuit is formed between the electrode and the workpiece, resulting in a voltage of 0 V, which is detected by the voltage sensor as a short circuit status. After the short circuit current is raised to 50 A, a program which has been implemented to restrict the current by varying the duty ratio is started to avoid the undesirable consequences of over-current, such as tungsten electrode burning or excessive melting of the workpiece, therefore improving the quality of the welding.

Once the short circuit current output is produced, the arc is initiated by lifting up the electrodes. Subsequently, the voltage between the electrodes and the workpiece rises to the arc voltage, which is considered as a successful arc ignition. If the voltage sensor records a sustained 0 V for a period exceeding 5 s, the protection program will be triggered, and the current output will be turned off. As a result, the welding arc of all types of output currents is initiated through contact arc initiation. With a successful arc initiation, the current is then switched to the pre-set value.

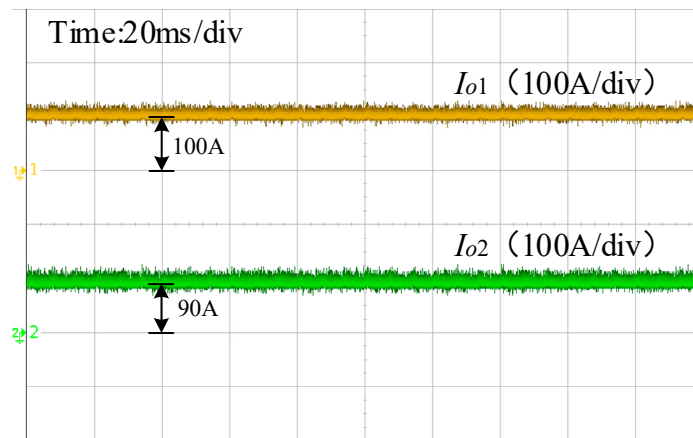
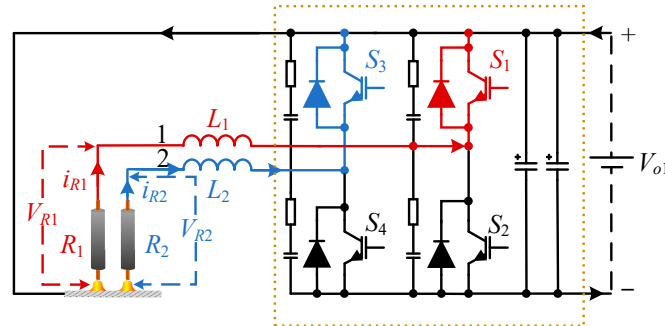
After the arc is initiated and reaches a steady state, maintaining a stable DC welding arc becomes relatively easier. However, when dealing with the AC arc welding process, it is necessary to utilize a dimensional arc unit. A dimensional arc unit is a reverse voltage generation module that generates a stable reverse voltage during the current polarity transformation, so that the space temperature and ionization degree are increased to meet the requirements of thermal emission and field-induced emission for arc stability.

Figure 13a shows two DC outputs, i.e., 100 and 90 A. The two DC waveforms are relatively stable, and the converter can achieve stable DC voltage. DC/DC mode is applied in the dual tungsten inert gas (TIG) welding process.

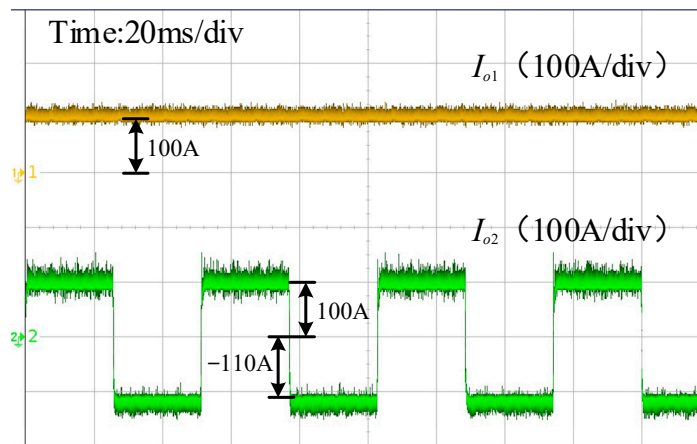
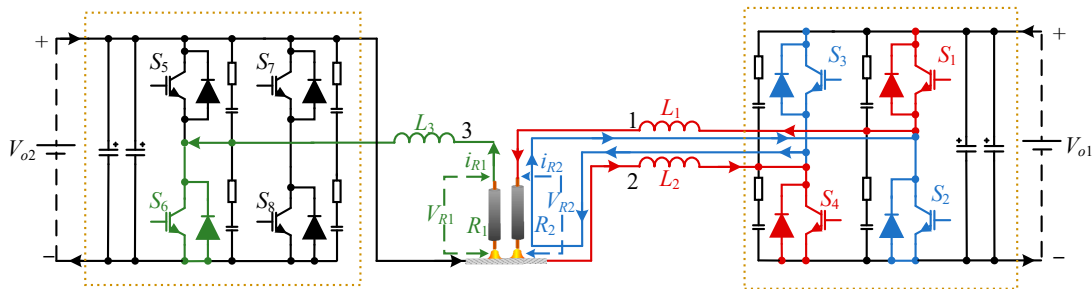
The dual tungsten–argon arc welding process utilizes the system that outputs two DC currents. In this process, the workpiece is connected to V_{o1+} , while the two tungsten poles are connected to electrode 1 and electrode 2 respectively, as demonstrated in Figure 13a.

Figure 13b shows one DC output and one AC output; the DC output is 100 A, the forward current of the AC output is 100 A, and the reverse current is 110 A. The DC current and AC current outputs are relatively stable. Moreover, the forward and reverse currents of the AC waveform can be independently adjusted. AC/DC mode is applied in the cross-coupling arc welding process.

This welding process represent a combination of AC MIG welding and DC TIG welding. In AC MIG welding, the two electrodes are connected to electrode 1 and electrode 2, respectively. For the DC TIG welding process, the workpiece is connected to V_{o2+} , while the tungsten electrode is connected to electrode 3, as demonstrated in Figure 13b.

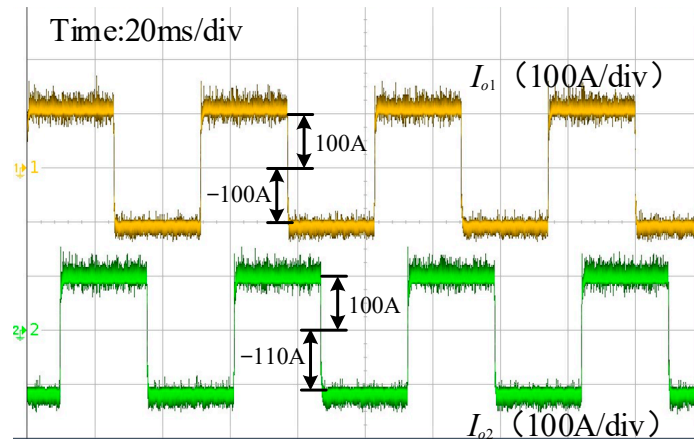
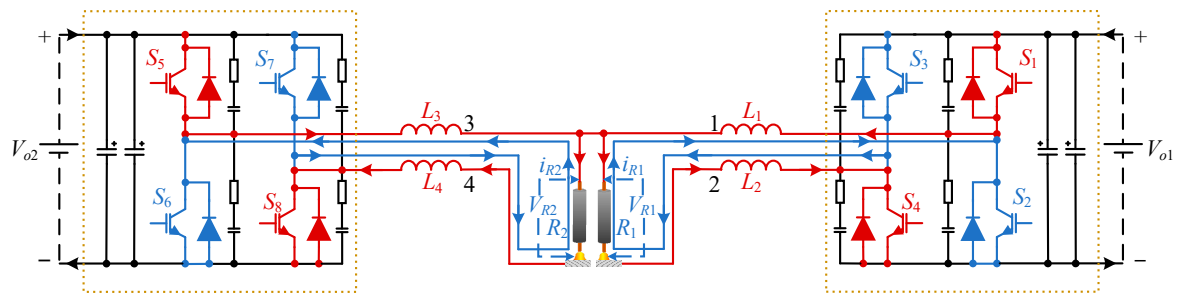


(a) DC/DC mode

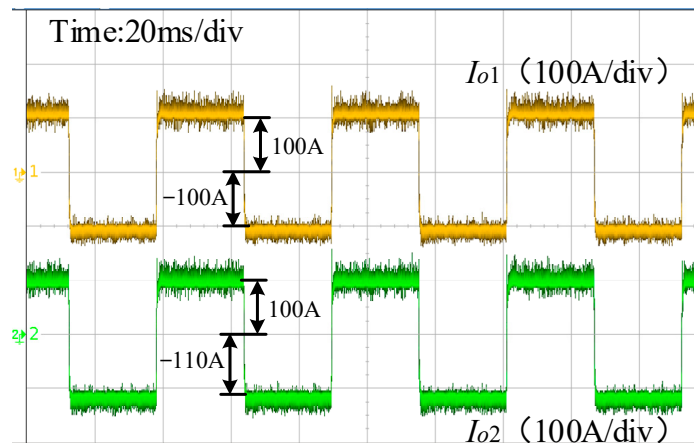


(b) AC/DC mode

Figure 13. Cont.



(c) AC/AC non-sync mode



(d) AC/AC sync mode

Figure 13. Experiment waveforms.

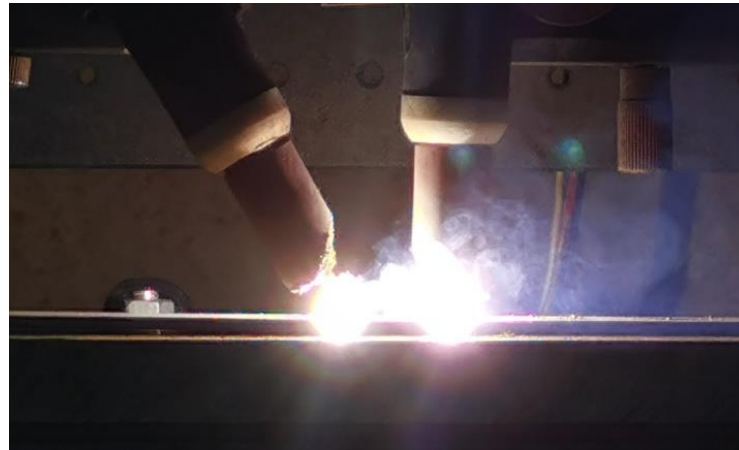
Figure 13c,d show the two AC outputs, where the forward and reverse currents of the AC outputs are 100 and 110 A, respectively. The converter can output two AC waveforms with the same phase and two AC waveforms with different phases, and the two AC waveforms are independently adjustable. AC/AC mode is applied in the dual variable polarity plasma arc welding process.

This welding process is a combination of AC plasma welding and AC TIG welding. For the AC plasma welding portion, the two electrodes are connected to electrode 1 and electrode 2, respectively, while in the AC TIG welding portion, the two electrodes are connected to electrode 3 and electrode 4, respectively. Since both AC plasma welding and AC TIG welding share the same tungsten electrode, electrode 1 and electrode 3 are connected to the tungsten electrode, as demonstrated in Figure 13c.

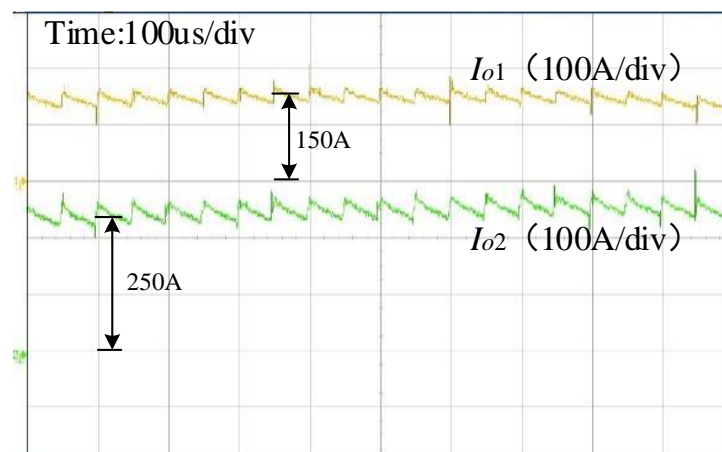
Both AC/AC non-sync mode and AC/AC sync mode are designed for the dual variable polarity plasma arc welding process. The selection of non-sync or sync current

can significantly impact the solidification process of the welding and, therefore, must be carefully considered.

After the current output experiments, the system was tested for actual welding. The dual TIG welding process was used as the welding arc for testing, as TIG welding is convenient to connect, the arc is easy to start, and TIG welding exists in all multi-electrode arc welding processes; the test results are shown in Figure 14.



(a) Dual TIG welding



(b) The corresponding waveforms of the dual TIG welding process

Figure 14. Actual welding experiment.

5. Conclusions

In this paper, a novel power-supply architecture for a multi-output welding power-supply system is proposed. This welding power supply comprises a three-phase rectifier unit, a full-bridge converter unit, a HF transformer, a rectifier unit, and a chopper converter unit. The three-phase rectifier unit, full-bridge converter unit, HF transformer, and rectifier unit convert the three-phase AC voltage into a low voltage, while the chopper converter unit serves as the key component, utilizing the low voltage to convert it into a specific current output. By switching different IGBTs in the chopper converter unit, the power supply can generate two DC currents or one AC current output.

Based on this power supply, a control method and closed-loop control model for the power-supply system is established. The power supply employs the PI control method to achieve closed-loop control, with PI parameters determined by calculations. The results indicate stability for the power supply.

The experimental prototype that includes two sets of the architecture is designed, enabling the power supply to output four DC and two AC currents. Experimental validation

demonstrates that the prototype can simultaneously output AC and DC currents with different values. The current of different outputs can be independently controlled, including the phase and frequency of AC current and the magnitude of forward and reverse currents. Furthermore, the stable output current meets actual production requirements, indicating its availability for arc initiation.

By generating the different types of current that this power supply outputs, various welding processes can be realized. We tested the dual TIG welding process for the welding arc, and the results show successful arc initiation.

For future work, research on multi-output power supplies for multi-electrode arc welding will focus on improving the current response speed and current output synchronization at high speeds to achieve higher AC current frequencies, as well as continue to advance the control methods of multi-output power-supply modules.

Author Contributions: Conceptualization, S.C.; Methodology, Y.Y.; Software, H.Z.; Validation, M.L.; Writing—original draft, J.Z. All authors have read and agreed to the published version of the manuscript.

Funding: This work was supported by National Natural Science Foundation of China (Hongyan Zhao, Grant No. 52205325).

Data Availability Statement: The data presented in this study are available in the article.

Conflicts of Interest: The authors declare no conflict of interest.

Abbreviations

The following abbreviations are used in this manuscript:

GMAW	Gas Metal Arc Welding
HF	High Frequency
AC	Alternate Current
DC	Direct Current
GTAW	Gas Tungsten Arc Welding
IGBT	Insulated Gate Bipolar Transistor
TIG	Tungsten Inert Gas Welding

References

1. Chen, S.J.; Feng, L.; Li, L.; Yin, S.; Zhang, S. Principle and parameter design of arc welding inverter using soft switching technique. *China Weld.* **1998**, *1*, 63–70.
2. Chen, J.S.; Lu, Y.; Li, X.R.; Zhang, Y.M. Gas tungsten arc welding using an arcing wire. *Weld. J.* **2012**, *91*, 261–269.
3. Chen, S.J.; Zhang, L.; Wang, X.P.; Wang, J. Stability of the cross-arc process—A preliminary study. *Weld. J.* **2015**, *94*, 158–168.
4. Lee, D.Y.; Leifsson, L.; Kim, J.; Lee, S.H. Optimization of hybrid tandem metal active gas welding using Gaussian process regression. *Sci. Technol. Weld. Join.* **2020**, *25*, 208–217. [[CrossRef](#)]
5. Zhang, Y.; Zhang, S.; Jiang, M.; Wu, L. Keyhole double-sided arc welding process. *J. Mater. Sci. Technol.* **2001**, *17*, 159–160. [[CrossRef](#)]
6. Li, K.H.; Chen, J.S.; Zhang, Y. Double-electrode GMAW process and control. *Weld. J.* **2007**, *86*, 231.
7. Kumar, K.; Chandra, D.S.; Masanta, M. Effect of Activated Flux on TIG Welding of 304 Austenitic Stainless Steel. *Mater. Today Proc.* **2019**, *18*, 4792–4798. [[CrossRef](#)]
8. Dong, S.; Jiang, F.; Xu, B.; Chen, S.J. Influence of Polarity Arrangement of Inter-Wire Arc on Droplet Transfer in Cross-Coupling Arc Welding. *Materials* **2019**, *12*, 3985. [[CrossRef](#)]
9. Ton, H. Physical properties of the plasma-MIG welding arc. *J. Phys. D Appl. Phys.* **1975**, *8*, 922–933. [[CrossRef](#)]
10. Guo, Y.; Pan, H.; Ren, L.; Quan, G. An investigation on plasma-MIG hybrid welding of 5083 aluminum alloy. *Int. J. Adv. Manuf. Technol.* **2018**, *98*, 1433–1440. [[CrossRef](#)]
11. Bai, Y.; Gao, H.; Qiu, L. Droplet transition for plasma-MIG welding on aluminium alloys. *Trans. Nonferrous Met. Soc. China* **2010**, *20*, 2234–2239. [[CrossRef](#)]
12. Chen, M.A.; Wu, C.S.; Li, S.K.; Zhang, Y.M. Analysis of active control of metal transfer in modified pulsed GMAW. *Sci. Technol. Weld. Join.* **2013**, *12*, 10–14. [[CrossRef](#)]
13. Ma, G.; Zhang, Y. A novel DE-GMAW method to weld steel tubes on simplified condition. *Int. J. Adv. Manuf. Technol.* **2012**, *63*, 147–153. [[CrossRef](#)]

14. Chen, S.; Zhang, S.; Huang, N.; Zhang, P.; Han, J. Droplet transfer in arcing-wire GTAW. *J. Manuf. Process.* **2016**, *23*, 149–156. [[CrossRef](#)]
15. Chen, S.; Zhang, L.; Men, G. Effect of Torch Height on Arc Stability in Divided-Arc Processes. *Weld. J.* **2016**, 47–56.
16. Huang, J.; Shi, Y.; Lu, L.; Zhu, M.; Zhang, Y.; Fan, D. Modeling and Decoupling Control Analysis for Consumable DE-GMAW. In *Robotic Welding, Intelligence and Automation; Lecture Notes in Electrical Engineering*; Springer: Berlin/Heidelberg, Germany, 2011; pp. 285–292.
17. Arita, H.; Morimoto, T.; Nagaoka, S.; Nakano, T. Development of Advanced 3-Electrode MAG High-Speed Horizontal Fillet Welding Process. *Weld. World* **2009**, *53*, 35–43. [[CrossRef](#)]
18. Wang, X.; Fan, D.; Huang, J.; Huang, Y. Numerical simulation of arc plasma and weld pool in double electrodes tungsten inert gas welding. *Int. J. Heat Mass Transf.* **2015**, *85*, 924–934. [[CrossRef](#)]
19. Lu, Z.; Dong, S.; Jiang, F.; Li, C. Analysis of Electrical Characteristics of Inter-wire Arc in Cross-Coupling Arc. *Chin. J. Mech. Eng.* **2019**, *32*, 22. [[CrossRef](#)]
20. Zhang, L.; Su, S.; Wang, J.; Chen, S.J. Investigation of arc behaviour and metal transfer in cross arc welding. *J. Manuf. Process.* **2019**, *37*, 124–129. [[CrossRef](#)]
21. Zhang, L.; Chen, S.; Song, Y.X. Metal Transfer in the Cross-Arc Welding Process. *Weld. J.* **2016**, *94*, 340–356.
22. Rezayi, S.; Iman Eini, H.; Hamzeh, M.; Bacha, S.; Farzamkia, S. Dual-output DC/DC boost converter for bipolar DC microgrids. *IET Renew. Power Gen.* **2019**, *13*, 1402–1410. [[CrossRef](#)]
23. Zhang, Z.; Xie, S.; Wu, Z.; Xu, J. Soft-switching and low conduction loss current-fed isolated bidirectional DC–DC converter with PWM plus dual phase-shift control. *J. Power Electron.* **2020**, *20*, 664–674. [[CrossRef](#)]
24. Hu, Y.; Xue, J.; Dong, C.; Jin, L.; Zhang, Z. Effect of Additional Shielding Gas on Welding Seam Formation during Twin Wire DP-MIG High-Speed Welding. *Appl. Sci.* **2018**, *8*, 1658. [[CrossRef](#)]
25. Xue, J.; Xu, M.; Huang, W.; Zhang, Z.; Wu, W.; Jin, L. Stability and Heat Input Controllability of Two Different Modulations for Double-Pulse MIG Welding. *Appl. Sci.* **2019**, *9*, 127. [[CrossRef](#)]
26. Yao, P.; Xue, J.; Zhou, K.; Wang, X.; Zhu, Q. Symmetrical transition waveform control on double-wire MIG welding. *J. Mater. Process. Technol.* **2016**, *229*, 111–120. [[CrossRef](#)]

Disclaimer/Publisher’s Note: The statements, opinions and data contained in all publications are solely those of the individual author(s) and contributor(s) and not of MDPI and/or the editor(s). MDPI and/or the editor(s) disclaim responsibility for any injury to people or property resulting from any ideas, methods, instructions or products referred to in the content.